$Bi_4LnNb_3O_{15}$ (Ln = La, Pr, Nd) and $Bi_4LaTa_3O_{15}$: New intergrowth Aurivillius related phases

Tapas Kumar Mandal [a], Saji Augustine [a], J. Gopalakrishnan [a,*], Ph. Boullay [b]

[a] *Solid State and Structural Chemistry Unit, Indian Institute of Science, Bangalore 560 012, India*
[b] *Laboratoire de Sciences des Procédés Céramiques et Traitements de Surface (CNRS UMR 6638), Université de Limoges, 123 Avenue Albert Thomas, F-87060 Limoges Cedex, France*

Abstract

We describe the synthesis and characterization of new intergrowth Aurivillius related phases, $Bi_4LnNb_3O_{15}$ (Ln = La, Pr, Nd) and $Bi_4LaTa_3O_{15}$. Both powder X-ray diffraction and electron microscopy investigations show that the compounds adopt orthorhombic structures with the cell parameters $a \sim 5.5$ Å, $b \sim 5.5$ Å and $c \sim 20.9$ Å, suggesting an ordered intergrowth structure that consists of $n = 1$ $[Bi_2NbO_6]^-$ and $n = 2$ $[Bi_2LnNb_2O_9]^+$ Aurivillius fragments which are stacked alternately along the c-axis. The oxides do not show a second harmonic generation (SHG) response toward 1064 nm laser radiation; they do not show a ferroelectric–paraelectric transition either between 30 and 900 °C in dielectric measurements, indicating a centrosymmetric structure. Optical absorption studies show that the intergrowth phases possess considerably smaller band gaps than the parent Nb_2O_5 and Ta_2O_5.

Keywords: A. oxides; A. layered compounds; C. X-ray diffraction; C. electron diffraction; C. electron microscopy; D. optical properties

1. Introduction

Among the several layered variants of the perovskite structure [1], the Aurivillius phases, $(Bi_2O_2)A_{n-1}B_nO_{3n+1}$ discovered in 1949 [2] continue to attract attention [3,4] in view of the ferroelectric properties of importance to developing non-volatile random access memories. Bi_2WO_6 ($n = 1$),

* Corresponding author. Tel.: +91 80 2293 2537; fax: +91 80 2360 1310.
E-mail address: gopal@sscu.iisc.ernet.in (J. Gopalakrishnan).

$Bi_2SrTa_2O_9$ ($n = 2$) and $Bi_4Ti_3O_{12}$ ($n = 3$) are some of the well-characterized Aurivillius phases. A special feature of the Aurivillius phases is that they form ordered intergrowth structures between adjacent n and $n + 1$ members. Ordered intergrowth Aurivillius phases were discovered by Kikuchi in 1976 [5] and it was further elaborated by Rao and coworkers [6,7]. Intergrowth Aurivillius phases corresponding to ($n = 2$) + ($n = 3$) composition ($Bi_7Ti_4NbO_{21} = Bi_3TiNbO_9 + Bi_4Ti_3O_{12}$) [5,8] as well as ($n = 3$) + ($n = 4$) composition ($Bi_9Ti_6CrO_{27} = Bi_4Ti_3O_{12} + Bi_5Ti_3CrO_{15}$) [6,7] have been well characterized by X-ray diffraction and high-resolution electron microscopy. Formation of ($n = 1$) + ($n = 2$) intergrowth structures has been reported for the compositions, $Bi_5TiNbWO_{15}$ [9], $Na_{0.5}Bi_{4.5}Nb_2WO_{15}$ [9], $Bi_5Ti_{1.5}W_{1.5}O_{15}$ [10] and $Bi_5Nb_3O_{15}$ [6], but no detailed structures have been published to date [11].

In an early study of the rare earth bismuth titanates $Bi_{4-x}Ln_xTi_3O_{12}$ (Ln = La, Pr, Nd and Sm) Wolfe and Newnham [12] have indicated that Bi/Ln substitution is possible in the perovskite slabs of the Aurivillius phases. Recently [4], the ferroelectric $Bi_{4-x}La_xTi_3O_{12}$-based capacitors have attracted considerable interest due to their excellent fatigue-free properties that has resulted in further literature on this system [13–16] (to mention only a few related to structural characterizations). Similar to this ($n = 3$) series of compounds, we believed that ($n = 1$) + ($n = 2$) intergrowth Aurivillius phases would exist for the composition, $Bi_4LnM_3O_{15}$ (Ln = La, Pr, Nd; M = Nb, Ta). Accordingly, we synthesized these phases by solid-state reaction and characterized their structure and properties by powder X-ray diffraction, electron microscopy, SHG response and optical absorption. The results of these investigations are presented in this paper.

2. Experimental

$Bi_4LnNb_3O_{15}$ (Ln = La, Pr, Nd) and $Bi_4LaTa_3O_{15}$ were synthesized by conventional solid-state reaction of the constituent oxides [Bi_2O_3, Ln_2O_3 (pre-dried at 950 °C) and Nb_2O_5/Ta_2O_5] at elevated temperatures. Powder X-ray diffraction (XRD) patterns were recorded using a Siemens D5005 powder diffractometer (Cu Kα radiation). Unit cell parameters were least-squares refined by the PROSZKI [17] program. Chemical compositions, synthesis conditions and lattice parameters of the oxides investigated in this study are summarized in Table 1.

Scanning electron microscopy (SEM) and energy dispersive X-ray (EDX) analysis were carried out using a JEOL JSM 5600 LV microscope equipped with a Link/ISIS system from Oxford Instruments. The electron microscopy investigations have been carried out on one of the samples ($Bi_4LaNb_3O_{15}$) using a JEOL 2010 microscope working at 200 kV and fitted with a double-tilt (±30°) rotating sample holder. The powder was crushed in an agate mortar to obtain small fragments that were put in a suspension in

Table 1
Chemical compositions, synthesis conditions and lattice parameters of $Bi_4LnM_3O_{15}$ (Ln = La, Pr, Nd; M = Nb, Ta)

Compound	Synthesis condition[a]	Lattice parameters (Å)		
		a	*b*	*c*
$Bi_4LaNb_3O_{15}$	810 °C/24 h	5.469(4)	5.471(2)	20.864(9)
$Bi_4PrNb_3O_{15}$	810 °C/24 h; 900 °C/48 h; 930 °C/24 h	5.464(1)	5.466(1)	20.865(4)
$Bi_4NdNb_3O_{15}$	810 °C/24 h; 900 °C/48 h; 930 °C/24 h	5.461(1)	5.462(1)	20.841(4)
$Bi_4LaTa_3O_{15}$	900 °C/24 h; 930 °C/24 h	5.476(3)	5.478(2)	20.820(6)

[a] Constituent oxides taken in stoichiometric proportion were reacted in air at the synthesis condition given.

alcohol. A drop of the suspension was then deposited and dried on a copper grid previously coated with a thin film of amorphous carbon. Powder second harmonic generation (SHG) test was carried out using 1064 nm laser radiation with an equipment similar to that used by Kurtz and Perry [18]. A pulsed Q-switched Nd:YAG laser (Spectra Physics DCR-II) with pulse duration of 8 ns was used in the experiments. Diffuse reflectance spectra of $Bi_4LaNb_3O_{15}$ and $Bi_4LaTa_3O_{15}$ were recorded using a Perkin Elmer Lambda 35 double-beam spectrometer over the spectral range 200–800 nm using MgO as standard. Reflectance data were collected and converted to absorbance. Band gap energies were estimated by Shapiro's method [19,20] by extrapolating the onset of absorption to the wavelength axis. The spectra were calibrated using Nb_2O_5 and Ta_2O_5 as standards.

3. Results and discussion

We investigated the formation of (n = 1) + (n = 2) intergrowth Aurivillius phases for the compositions $Bi_4LnNb_3O_{15}$ (Ln = La, Pr, Nd) and $Bi_4LaTa_3O_{15}$ by reacting the component oxides in air at elevated temperatures. Single-phase materials similar to $Bi_5Nb_3O_{15}$ were obtained readily at 810–930 °C. SEM and EDX analysis (Fig. 1) of $Bi_4LaNb_3O_{15}$ and $Bi_4LaTa_3O_{15}$ showed the single-phase nature and the expected metal atom ratios. Powder XRD patterns (Fig. 2) showed that all the phases possess orthorhombic structures similar to that of parent $Bi_5Nb_3O_{15}$. Powder XRD data (Tables 1 and 2) show

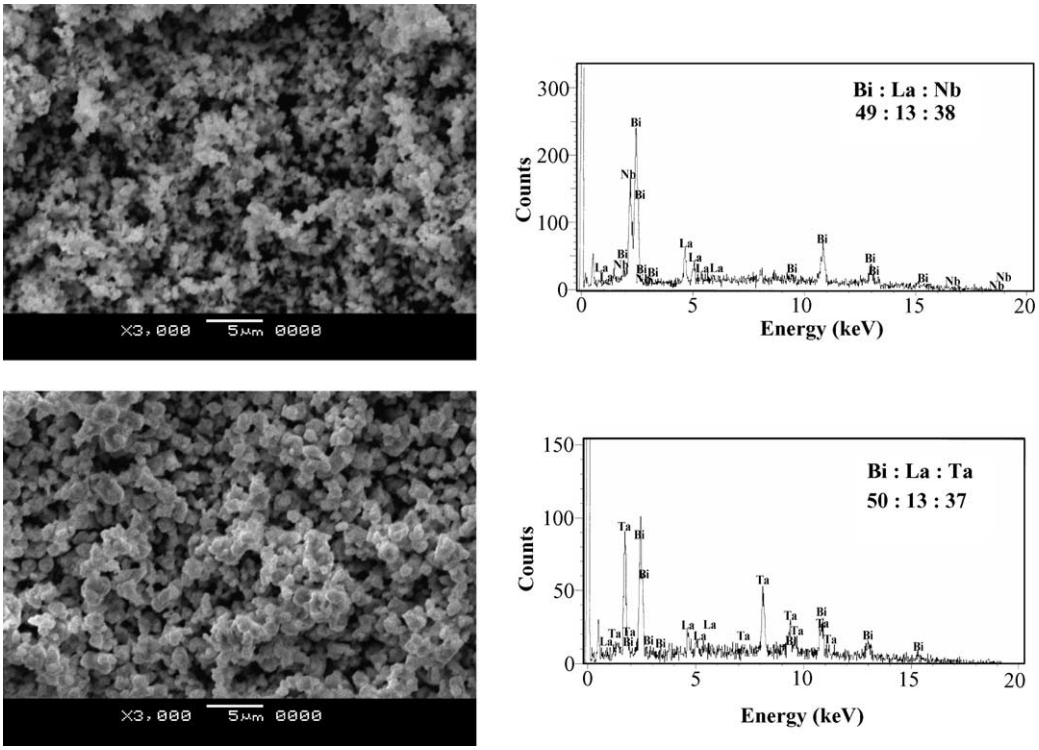

Fig. 1. SEM images of $Bi_4LaNb_3O_{15}$ (top) and $Bi_4LaTa_3O_{15}$ (bottom). The corresponding EDX data are shown in the right side panels. The average metal atom ratios are indicated.

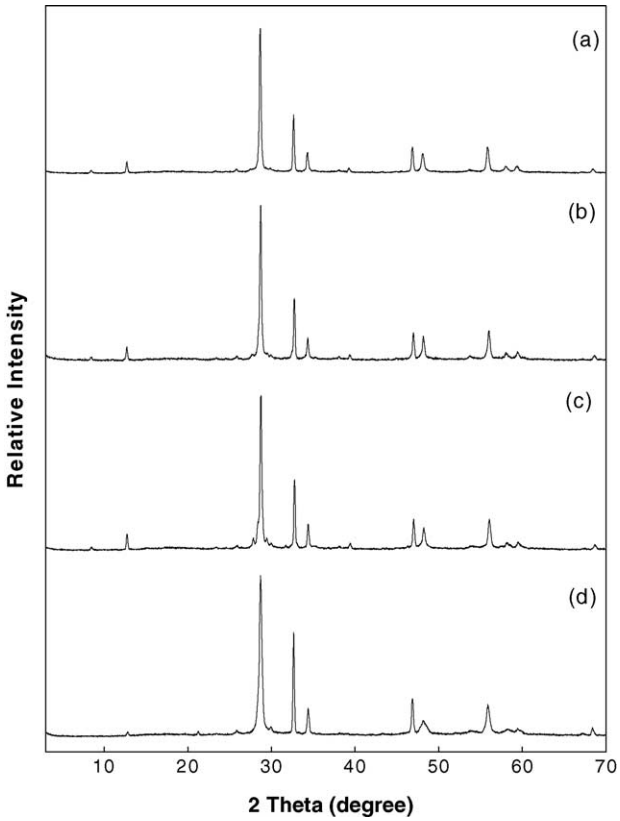

Fig. 2. Powder XRD patterns of: (a) $Bi_4LaNb_3O_{15}$, (b) $Bi_4PrNb_3O_{15}$, (c) $Bi_4NdNb_3O_{15}$ and (d) $Bi_4LaTa_3O_{15}$.

Table 2
Powder XRD data for $Bi_4LaTa_3O_{15}$

h	k	l	d_{obs} (Å)	d_{cal} (Å)	I_{obs}
0	0	3	6.900	6.940	3
1	1	4	3.107	3.107	100
0	0	7	2.979	2.974	3
0	2	0	2.739	2.739	65
2	0	0	2.739	2.739	65
0	0	8	2.605	2.603	19
2	2	0	1.937	1.936	23
0	2	8	1.887	1.887	12
2	0	8	1.887	1.886	12
1	1	11	1.701	1.701	2
3	1	4	1.643	1.644	19
1	1	12	1.582	1.583	5
2	2	8	1.553	1.554	5
0	0	15	1.391	1.388	3
4	0	0	1.370	1.370	8

a = 5.476(3) Å, b = 5.478(2) Å, c = 20.820(6) Å.

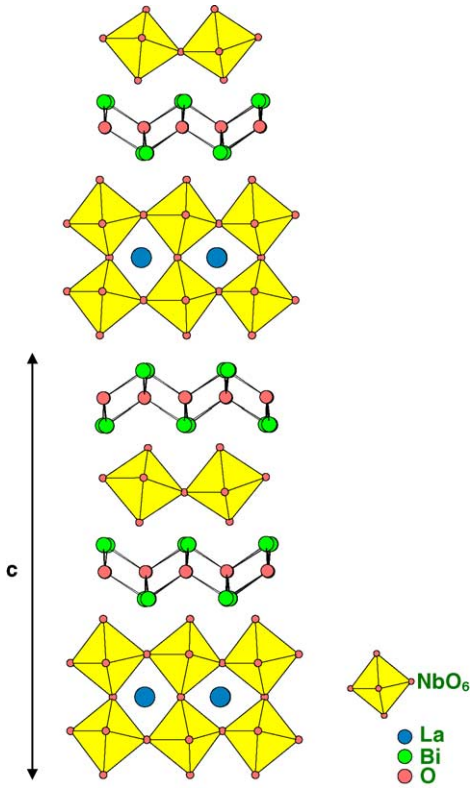

Fig. 3. Schematic representation of the structure of (n = 1) + (n = 2) ordered intergrowth Aurivillius phase, e.g. $Bi_4LaNb_3O_{15}$.

that all the compounds adopt orthorhombic structures with the cell parameters $a \sim 5.5$ Å, $b \sim 5.5$ Å and $c \sim 20.9$ Å suggesting that the structure of $Bi_4LnM_3O_{15}$ most likely consists of alternating $[Bi_2MO_6]^-$ (∼8.4 Å thick) and $[Bi_2LnM_2O_9]^+$ (∼12.6 Å thick) sheets stacked one over the other along the c-direction. Fig. 3 shows a schematic drawing of such an (n = 1) + (n = 2) ordered intergrowth phase.

Nonetheless, as indicated in the proposed general structural model for Aurivillius phases [21], the existence of structural distortions would impose to consider twice the value of the c parameter (here $c \sim 42$ Å) for such an ordered intergrowth phase. The occurrence of $c \sim 21$ Å only can be understood by the fact that this expected doubling of the c parameter is almost exclusively due to opposite rotations of the oxygen octahedral network from one perovskite block to the other (see Fig. 3 as an illustration and Refs. [11,21]). Considering that oxygen atoms did not give a strong contribution to the powder XRD data, we have performed ED investigations to check this point. As shown in Fig. 4, the selected SAED patterns support the lattice parameters obtained from the powder XRD data and, in addition, the [−2,1,0] zone axis pattern (Fig. 4c) shows extra spots that correspond to the expected doubling of the c-axis ($c \sim 42$ Å) with a I-centering of the lattice. The observed conditions limiting the reflections are compatible with the space groups *I2cb* (SG no. 45:cab) and *Imcb* (SG no. 72:cab), which belong to the possible space groups predicted, respectively, for a polar [21] and non-polar [22] orthorhombic Aurivillius intergrowth. As a whole, the obtained SAED patterns and the corresponding image (Fig. 4d) obtained by high-resolution electron microscopy for $Bi_4LaNb_3O_{15}$ are consistent with a layered (n = 1) + (n = 2) intergrowth structure. However, a careful examination of the HREM image (Fig. 4d) reveals that the contrast

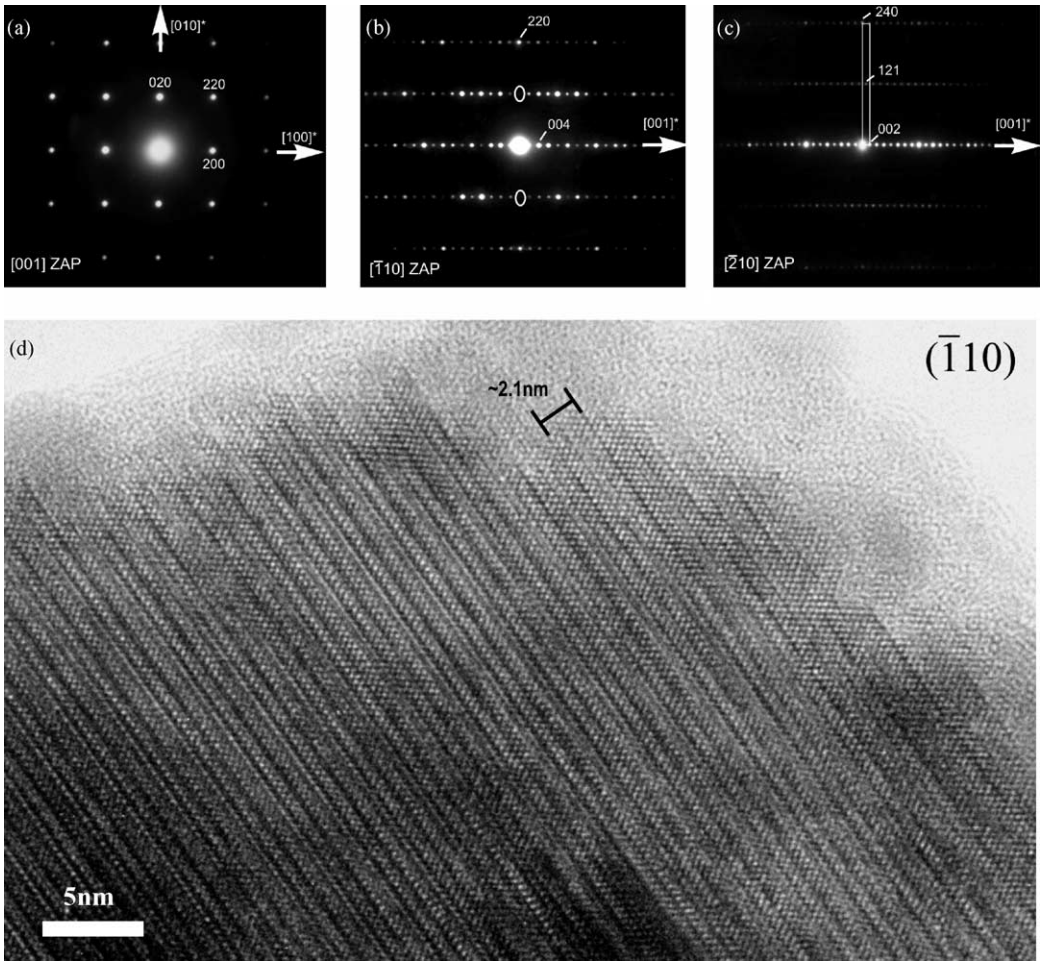

Fig. 4. Transmission electron microscopy data for $Bi_4LaNb_3O_{15}$. Selected SAED patterns corresponding to the zone axis pattern: (a) [0 0 1], (b) [−1,1,0] and (c) [−2,1,0]. These patterns indicate a I-centered orthorhombic lattice with cell parameters $a \sim 5.4$ Å, $b \sim 5.4$ Å and $c \sim 42$ Å. The doubling of the c parameter as compared to the value obtained by XRPD data is clearly evidenced in the [−2,1,0] ZAP in (c). In (d), a high-resolution image associated to the ED pattern presented in (b) reveals the ordered intergrowth structure.

due to (Bi_2O_2) slabs in $Bi_4LaNb_3O_{15}$ is not exactly the same as that observed for a typical $(n = 1) + (n = 2)$ ordered intergrowth structure such as $Bi_5Ti_{1.5}W_{1.5}O_{15}$ [11]. Instead, it looks like that every alternate (Bi_2O_2) slabs have joined with the perovskite slabs. This could be due to substitution of La for Bi in alternate (Bi_2O_2) slabs rearranging them to fluorite-like slabs. Evidence for Bi/La ordering in the *a–b* plane observed in the ED patterns of certain crystals lends support to the above model. A determination of the actual crystal structure of $Bi_4LaNb_3O_{15}$ would confirm the structural model.

Considering that most of the Aurivillius phases are ferroelectric materials and adopt non-centrosymmetric structures, we investigated $Bi_4LnM_3O_{15}$ by second harmonic generation (SHG). None of these oxides, however, showed a positive SHG response toward 1064 nm laser radiation. Interestingly, the corresponding $Bi_5Nb_3O_{15}$ did show a distinct SHG response toward 1064 nm laser radiation. These

results suggest that while $Bi_5Nb_3O_{15}$ is likely to adopt a non-centrosymmetric intergrowth structure, the lanthanide-substituted derivatives ($Bi_4LnM_3O_{15}$) are most likely centrosymmetric and thus, in the case of $Bi_4LaNb_3O_{15}$, would indicate that the correct space group is *Imcb* (SG no.72:cab). Dielectric constant measurements by impedance spectroscopy also show that there is no ferroelectric–paraelectric transition between 30 and 900 °C in $Bi_4LaNb_3O_{15}$. Accordingly, the substitution of La for Bi appears to destroy the non-centrosymmetric structure. Similar results have been obtained for $Bi_4Ti_3O_{12}$ and $Bi_2La_2Ti_3O_{12}$ [4,13–16]: the latter adopts a centrosymmetric structure, in contrast to $Bi_4Ti_3O_{12}$ [23], a well-known ferroelectric.

We investigated the optical absorption spectrum of the representative members of $Bi_4LnM_3O_{12}$, considering the recent interest in Aurivillius phases as photocatalysts working under visible light [24]. The spectra (Fig. 5) clearly show that both $Bi_4LaNb_3O_{15}$ and $Bi_4LaTa_3O_{15}$ possess distinctly smaller band gaps than the parent Nb_2O_5 and Ta_2O_5. Thus the estimated band gaps for $Bi_4LaNb_3O_{15}$ and $Bi_4LaTa_3O_{15}$ are 2.7 and 2.8 eV, respectively. The corresponding band gaps for Nb_2O_5 and Ta_2O_5 are 3.0 and 4.0 eV, respectively. The smaller band gaps suggest that both $Bi_4LaNb_3O_{15}$ and $Bi_4LaTa_3O_{15}$ would be potential visible light driven photocatalysts similar to $PbBi_2Nb_2O_9$ [24]. The significant lowering of band gaps in the Bi-compounds is most likely due to a strong hybridization of Bi:6s with O:2p which would render the band gap transition to Bi:6s → $Nb^V/Ta^V:d^0$ in the ionic limit, instead of the usual O:2p → $Nb^V/Ta^V:d^0$ transition in d^0 oxides without Bi^{III}/Pb^{II}. Further investigations of the exact structure and optical properties of the intergrowth Aurivillius phases reported here would be fruitful.

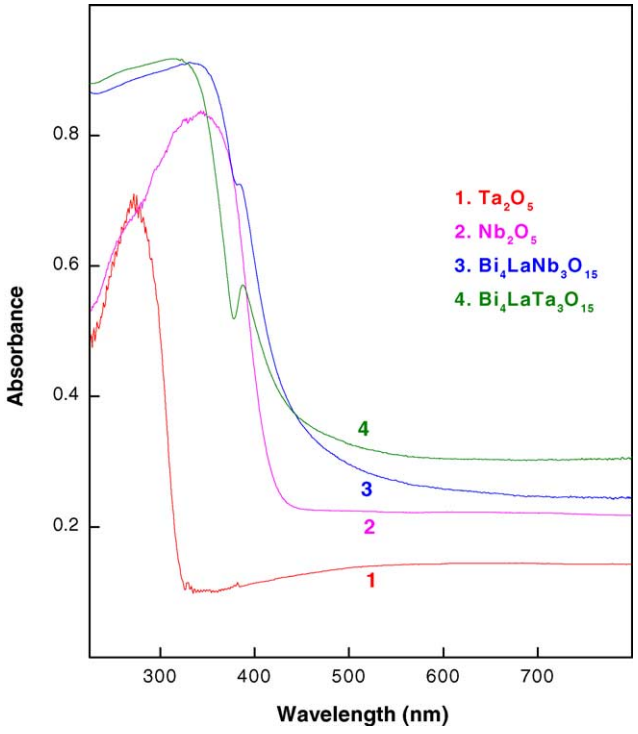

Fig. 5. UV–vis diffuse reflectance spectra of $Bi_4LaNb_3O_{15}$ and $Bi_4LaTa_3O_{15}$. For comparison, the corresponding spectra for Nb_2O_5 and Ta_2O_5 are also shown.

4. Conclusions

New Aurivillius related $(n = 1) + (n = 2)$ intergrowth phases corresponding to the formulas $Bi_4LnNb_3O_{15}$ (Ln = La, Pr, Nd) and $Bi_4LaTa_3O_{15}$ have been synthesized and characterized. Both powder XRD and ED investigations reveal the occurrence of an ordered intergrowth structure. The lack of SHG activity of the new phases stands in contrast to the distinct SHG response of the parent $Bi_5Nb_3O_{15}$. The new oxides possess significantly smaller band gaps than Nb_2O_5/Ta_2O_5 and this could render these materials useful for visible light driven photocatalytic applications.

Acknowledgements

We thank the Department of Science and Technology (DST), Government of India for support of this research work. We also thank Professor P.K. Das, Department of Inorganic and Physical Chemistry, Indian Institute of Science, Bangalore, for SHG measurements and Dr. Ram Seshadri, Materials Department, UCSB, U.S.A., for his valuable contribution to this work.

References

[1] R.H. Mitchell, Perovskites: Modern and Ancient, Almaz Press, Thunder Bay, Canada, 2002.
[2] (a) B. Aurivillius, Ark. Kemi 1 (1949) 463;
(b) B. Aurivillius, Ark. Kemi 2 (1950) 519.
[3] C. A-Paz de Araujo, J.D. Cuchiaro, L.D. McMillan, M.C. Scott, J.F. Scott, Nature 374 (1995) 627.
[4] B.H. Park, B.S. Kang, S.D. Bu, T.W. Noh, J. Lee, W. Jo, Nature 401 (1999) 682.
[5] T. Kikuchi, J. Less-Common Met. 48 (1976) 319.
[6] J. Gopalakrishnan, A. Ramanan, C.N.R. Rao, D.A. Jefferson, D.J. Smith, J. Solid State Chem. 55 (1984) 101.
[7] G.N. Subbanna, T.N. Guru Row, C.N.R. Rao, J. Solid State Chem. 86 (1990) 206.
[8] S. Horiuchi, T. Kikuchi, M. Goto, Acta Crystallogr. A 33 (1977) 701.
[9] T. Kikuchi, A. Watanabe, K. Uchida, Mater. Res. Bull. 12 (1977) 299.
[10] L.A. Shebanov, V.G. Osipyan, E.Z. Freidenfield, Izv. Akad. Nauk SSSR, Neorg. Mater. 18 (1982) 305.
[11] Note that the crystal structure of $Bi_5Ti_{1.5}W_{1.5}O_{15}$ has been recently established, J. Tellier, Ph. Boullay, N. Créon, D. Mercurio, Solid State Sci., submitted for publication. The crystal structure of $Bi_5TiNbWO_{15}$ has recently been solved, after this manuscript has been submitted: A. Snedden, D.O. Chaikin, V.A. Dolgikh, P. Lightfoot, J. Solid State Chem. 178 (2005) 180.
[12] R.W. Wolfe, R.E. Newnham, J. Electrochem. Soc. 116 (1969) 832.
[13] J. Gopalakrishnan, T. Sivakumar, K. Ramesha, V. Thangadurai, G.N. Subbanna, J. Am. Chem. Soc. 122 (2000) 6237.
[14] C.H. Hervoches, P. Lightfoot, Solid State Chem. 153 (2000) 66.
[15] N.C. Hyatt, J.A. Hriljac, T.P. Comyn, Mater. Res. Bull. 38 (2003) 837.
[16] M.W. Chu, M.T. Caldes, L. Brohan, M. Ganne, A. Marie, O. Joubert, Y. Piffard, Chem. Mater. 16 (2004) 31.
[17] W. Losocha, K. Lewinski, J. Appl. Crystallogr. 27 (1994) 437.
[18] S.K. Kurtz, T.T. Perry, J. Appl. Phys. 39 (1968) 3797.
[19] I.P. Shapiro, Opt. Spektrosk. 4 (1958) 256.
[20] H.W. Eng, P.W. Barnes, B.M. Auer, P.M. Woodward, Solid State Chem. 175 (2003) 94.
[21] Ph. Boullay, G. Trolliard, D. Mercurio, J.M. Perez-Mato, L. Elcoro, J. Solid State Chem. 164 (2002), 252 and 261.
[22] L. Elcoro, J.M. Perez-Mato, Z. Izaola, Ph. Boullay, D. Mercurio, Ferroelectrics 305 (2004) 79.
[23] C.H. Hervoches, P. Lightfoot, Chem. Mater. 11 (1999) 3359.
[24] H.G. Kim, D.W. Hwang, J.S. Lee, J. Am. Chem. Soc. 126 (2004) 8912.